^{1}H NMR Studies of Synthetic Peptide Analogues of Calcium-Binding Site III of Rabbit Skeletal Troponin C: Effect on the Lanthanum Affinity of the Interchange of Aspartic Acid and Asparagine Residues at the Metal Ion Coordinating Positions†

Brian J. Marsden, Robert S. Hodges, and Brian D. Sykes*

Department of Biochemistry and Medical Research Council of Canada Group in Protein Structure and Function, University of Alberta, Edmonton, Alberta, Canada T6G 2H7

Received September 29, 1987; Revised Manuscript Received January 20, 1988

ABSTRACT: The present work determines the contribution of liganding aspartic acid (Asp) residues, at the +X, +Y, and +Z metal ion coordinating positions, to the lanthanum(3+) (La^{3+}) ion binding affinity of synthetic analogues of calcium-binding site III of rabbit skeletal troponin C. Eight 13-residue synthetic analogues were prepared by solid-phase synthesis; the primary sequences of these analogues represent all possible combinations having aspartic acid and asparagine at the +X, +Y, and +Z positions. High-field proton nuclear magnetic resonance (NMR) spectroscopy was used to monitor the binding of the La^{3+} ion to each of the analogues. Comparison of the chemical shift changes showed large variations in the magnitude of the shift; these were reflected in the La^{3+} ion association constants determined for each analogue. The association constants ranged from 9.1×10^2 M^{-1} to 2.5×10^5 M^{-1}. It was observed that those analogues with the larger number of acidic residues to coordinate the La^{3+} ion yielded the higher association constants. The La^{3+} ion binding results demonstrate that the Asp residues at the positions of study contribute equally and in an additive manner to the association constant and that the presence of neighboring Asp residues at either the +X and +Y, the +Y and +Z, or the +X and +Y and +Z metal ion coordinating positions introduced dentate–dentate repulsion, which acts as to detract from the La^{3+} ion association constant of the analogues.

Calcium plays an important role in many biological systems, often acting as a second messenger (Kretsinger, 1980; Seamon & Kretsinger, 1983), where it effects a structural change in regulatory proteins such as troponin C (Ebashi et al., 1968) and calmodulin (Cheung, 1970; Kakiuchi & Yamazaki, 1970). Comparison of the primary sequence of these proteins reveals that the calcium-binding sites consist of highly homologous regions (Barker et al., 1978; Vogt et al., 1979; Reid & Hodges, 1980; Gariépy & Hodges, 1983). Each calcium-binding site exists in a helix–loop–helix arrangement 31 residues in length; this arrangement has been designated the "EF hand"[1] (Kretsinger & Nockolds, 1973).

The calcium-binding proteins are known to have from one to four of the EF-hand type calcium-binding sites (Kretsinger, 1980; Seamon & Kretsinger, 1983) and to have calcium affinities that range from 10^4 to 10^9 M^{-1}. In some proteins such as troponin C, which bind 4 mol of calcium/mol of protein, there are two distinct classes of sites; there are two high-affinity calcium sites which bind magnesium competitively, and there are also two lower affinity calcium-selective sites (Potter & Gergely, 1975).

The liganding of the calcium(2+) ion (Ca^{2+}) occurs within the 12-residue loop region. The Ca^{2+} ion is coordinated by the side-chain carboxyl and carbonyl oxygen atoms of Asx and Glu residues at the 1-, 3-, 5-, 9-, and 12-positions as well as the backbone carbonyl of residue 7. These dentates are in an almost octahedral arrangement about the calcium ion, with the residues at positions 1 and 9 occupying the ±X coordinates, 3 and 7 the ±Y coordinates, and 5 and 12 the ±Z coordinates of the Cartesian framework (Kretsinger & Nockolds, 1973; Herzberg et al., 1987; Satyshur et al., 1988).

It is expected that the calcium affinity of a site is determined primarily by the sequence of the loop region. This can be influenced by side-chain interactions with the calcium ion for the residues at the liganding positions, by contributions to the conformational changes that occur within the loop region upon binding calcium, or by interactions with other parts of the protein.

An ideal approach to understanding the affinity of a site in a calcium-binding protein would be to study the contribution of each residue in the site to either the residue–cation interaction or to the conformation of the loop. Such an approach can now be realized with the application of site-specific mutagenesis techniques to these proteins (Brodin et al., 1987). This approach, although being extremely powerful, is complicated due to the fact that one is attempting to study the effect of the change of a single amino acid residue in a calcium-binding site of 31 residues within a protein of 159 residues comprising a total of four calcium-binding sites, as would be the case for a study of TnC.

† This investigation was supported by a research grant from the Medical Research Council of Canada and a AHFMR fellowship (B.J.M.).

* Address correspondence to this author at the Department of Biochemistry.

[1] Abbreviations: AcSTnC(103–115)amide, synthetic N-terminal-acetylated rabbit skeletal troponin C fragment, residues 103–115, with a C-terminal amide; Boc, *tert*-butyloxycarbonyl; DCC, dicyclohexylcarbodiimide; D_2O, deuterium oxide; DSS, sodium 4,4-dimethyl-4-silapentane-1-sulfonate; EDTA, ethylenediaminetetraacetic acid; "EF hand", Kretsinger's abbreviation of the second calcium-binding domain of carp parvalbumin (this site is thought to represent a typical calcium-binding domain); HOBT, 1-hydroxybenzotriazole; HPLC, high-performance liquid chromatography; TFA, trifluoroacetic acid; TnC, calcium-binding unit of skeletal muscle troponin; Tos, *p*-toluenesulfonyl.

0006-2960/88/0427-4198$01.50/0

The use of natural fragments represents an alternate approach and one that has been used in several studies (Leavis et al., 1978; Derancourt et al., 1978), but often neither the size nor the choice of fragments can be easily controlled.

The chemical synthesis of a calcium-binding unit allows specific modifications or substitutions of any residue, and hence the contribution of any residue to the conformation of the site or complexation of the calcium ion to be studied. This approach was first developed by our group using synthetically prepared analogues to study site III of rabbit skeletal troponin C (Reid et al., 1980, 1981; Gariépy et al., 1982) and has since been adopted by other groups to study similar calcium-binding sites (Kanellis et al., 1983; Marchiori et al., 1983; Pavone et al., 1984; Borin et al., 1985; Buchta et al., 1986; Malik et al., 1987). Earlier work by our group has shown that the binding of metal ions to synthetic 13-residue analogues representing just the loop region of a calcium-binding site can be studied by using high-field ^1H nuclear magnetic resonance (NMR) spectroscopy and the combination can be used to probe the events that occur upon binding metal ions in great detail (Gariépy et al., 1983, 1985; Marsden et al., 1987). In these studies lanthanum(3+) ion (La^{3+}) is used as a Ca^{2+} ion analogue because of the increased affinity of calcium-binding sites for this ion due to the +3 charge.

In this paper we focus on the determination of the differences in the side chain–cation interaction between Asp and Asn liganding residues. We report the synthesis of eight analogues, the primary sequences of which are shown in Table I, of the high-affinity site III of rabbit skeletal troponin C and their La^{3+} ion binding affinities as determined by high-field ^1H NMR spectroscopy. The analogues synthesized represent all the possible combinations of Asp and Asn at the +X, +Y, and +Z coordinating positions (positions 1, 3, and 5 within the loop sequence). This has allowed the contribution of the Asp residues at each of these liganding positions to the lanthanum-binding affinity to be determined.

Experimental Procedures

Materials. Protected amino acid derivatives and other reagents used for the synthesis were described elsewhere (Reid et al., 1981). Lanthanum chloride was obtained from Alfa Inorganics–Ventron (Beverly, MA). Deuteriated imidazole was obtained from MSD Isotopes (Montreal, Canada). Deuterium oxide (99.96%) was obtained from Aldrich Chemical Co. (Milwaukee, WI).

Preparation of Analogues of STnC(103–115). The peptides were synthesized by stepwise solid-phase peptide synthesis on a Beckman 990 peptide synthesizer; the synthesis and cleavage from the support were performed as previously described (Reid et al., 1981) with the following exceptions: the coupling of the Boc-Asn residue was performed by symmetric anhydride coupling, and the Boc-Arg(Tos) residue was dissolved in a minimum of dimethyl formamide to aid dissolution and coupled with DCC and HOBT. The C-terminal residue was coupled to a benzhydrylamine resin support to generate a neutral C-terminal amide on the peptide. Because the first eight amino acids are common to all of the analogues, a large-scale preparation of the octapeptide was performed and the resin divided at each point where a desired substitution was required. This was repeated until all eight analogues had been synthesized.

The crude peptides were initially purified by high-performance liquid chromatography (HPLC) on a SynChropak Q300 ion-exchange column (Linden, IN: 250 × 4.1 mm i.d.). This is an essential step in the purification of the peptides, because it is known that hydrofluoric acid cleavage of peptides with an Asp-Gly sequence from the resin can produce a succinimide byproduct, which cannot be easily separated from the desired product by reverse-phase liquid chromatography (Barany & Merrifield, 1980; McFadden & Clark, 1986) but can be separated on the basis of charge by ion-exchange chromatography. Prior to purification by ion-exchange chromatography the pH of the peptide solution must be kept below pH 7.0, because the succinimide derivative undergoes rapid hydrolysis under basic conditions to produce α- and β-aspartyl peptides which cannot be easily separated chromatographically. The crude peptides were dissolved in 5 mM KH_2PO_4, pH 6.5, buffer, and the sample pH was readjusted to pH 6.5 with 0.1 M KOH. The sample was centrifuged to partition any particulate matter. Aliquots of the supernatent were then injected onto the column. A linear AB gradient was constructed by using 5 mM (buffer A) and 1 M (buffer B) KH_2PO_4 buffers adjusted to pH 6.5. The program used to isolate pure peptides N, I, II, and III was as follows: time 0, 80% A/20% B; linear gradient from 80% A/20% B to 65% A/35% B, at 30 min; linear gradient from 65% A/35% B to 80% A/20% B, at 35 min (gradient rate of 5 mM/min); and equilibration with 80% A/20% B, until 40 min. For peptides IV, V, VI, and VII the program was as follows: time 0, 85% A/15% B; linear gradient from 85% A/15% B to 75% A/25% B, at 30 min; linear gradient from 75% A/25% B to 85% A/15% B, at 35 min (gradient rate of 3.3 mM/min); and equilibration with 85% A/15% B, until 40 min. The flow rate was 1 mL/min, and the absorbance was recorded at 220 nm by using a 10-mm path cell. The major peak obtained for all the analogues was collected, pooled, and desalted on an HPLC preparative reverse-phase C-18 SynChropak RP-P column (Linden, IN; 250 × 10.0 mm i.d.). The peptide was dissolved in 0.1% TFA/water and the pH adjusted to 2.5 with 1 M HCl. Aliquots of the peptide were injected onto the column and eluted as a single peak by using the following linear AB gradient: time 0, 100% A; for 10 min; linear gradient 100% A to 80% A/20% B, at 15 min; linear gradient from 80% A/20% B to 65% A/35% B, at 30 min (gradient rate of 1% B/min); linear gradient from 65% A/35% B to 100% A, at 35 min; and equilibration with 100% A, until 40 min. The composition and concentration of the pure peptides were determined by amino acid analysis.

Preparation of ^1H NMR Samples. The metal-free spectrum of peptide II was recorded with a sample volume of 500 μL, and those of the other peptides were recorded with sample volumes of 600 μL of 20 mM deuteriated imidazole and 100 mM KCl at pH 6.5. The peptide samples were lyophilized from D_2O (99.96%, 3 × 250 μL) to reduce the HDO content. Prior to each La^{3+} titration three aliquots of 5 μL of each peptide solution were removed for concentration determination by amino acid analysis.

Amino Acid Analyses and Peptide Concentration Determinations. Aliquots (3 × 5 μL) of each peptide were removed prior to the La^{3+} titrations and added to 200 μL of 6 M HCl containing 1% phenol for hydrolysis in evacuated sealed tubes at 110 °C for 72 h; these samples were then evaporated to dryness, redissolved in 100 μL of 200 mM sodium citrate, pH 2.2, and eluted through an 8% cross-linked sulfonated polystyrene cation-exchange resin (Durram DC4A; 8-μm particle size; Durram Dionex D-500 amino acid analyzer) with the following series of buffers: 200 mM sodium citrate (pH 3.25), 200 mM sodium citrate (pH 4.25), and 200 mM sodium citrate/900 mM NaCl (pH 7.9). Concentration determinations were made by comparing peak areas with those obtained from standard sets of the amino acids (8 nmol each).

Proton NMR Experiments. The ^1H NMR spectra were recorded on either a Nicolet NT-300 WB spectrometer for peptide II or a Varian XL-400 spectrometer for the other peptides. The acquisition parameters for peptide II were as follows; probe size = 5 mm; peptide concentration = 1.88 mM; sample volume = 500 μL; spectral width = ±1200 Hz/16K data points; pulse length = 8.7 μs (≅90°); low-pass filter = Bessel (±3000 Hz) with quadrature phase detection; number of transients = 256; HDO suppression = continuous homonuclear decoupling; internal standard = methyl resonance of 4,4-dimethyl-4-silapentane-1-sulfonate (DSS); resolution enhancement = Lorentzian to Gaussian. The acquisition parameters for the other peptides were as follows: sample volume = 600 μL; peptide concentration for peptide I = 1.36 mM, for peptide N = 1.70 mM, for peptide III = 1.09 mM, for peptide IV = 1.19 mM, for peptide V = 3.15 mM, for peptide VI = 1.36 mM, and for peptide VII = 0.47 mM; spectral width = 3200 Hz/16000 data points; pulse length = 17 μs (≅90°); low-pass filter = ±1800 Hz with quadrature phase detection; number of transients = 256; HDO suppression = continuous homonuclear decoupling; internal standard = methyl resonance of 4,4-dimethyl-4-silapentane-1-sulfonate (DSS); resolution enhancement = Lorentzian to Gaussian.

Metal Ion Analysis. The lanthanum solution used in this study was prepared from reagent grade $LaCl_3 \cdot 5H_2O$ dissolved in 20 mM deuteriated imidazole and 100 mM KCl and adjusted to pH 6.50 with NaOD. The lanthanum content of the solution was determined by EDTA titration using xylenol orange as the end-point indicator (Lee & Sykes, 1980).

Calculation of the Lanthanum Binding Constants. The La^{3+} binding constant of a peptide was calculated by assuming that the peptide bound two metal ions, the first metal ion being coordinated by the six ligands of the loop and a nonspecific interaction to the second metal ion; the interaction with the first metal ion was stronger than that with the second. The equation for the interaction of the peptide with two metal ions is

$$P + M \underset{K_{d1}}{\rightleftharpoons} PM + M \underset{K_{d2}}{\rightleftharpoons} PM_2$$

$$K_{d1} = [P][M]/[PM] \quad (1)$$

$$K_{d2} = [PM][M]/[PM_2] \quad (2)$$

where [P] = concentration of free peptide, [M] = concentration of free metal, [PM] = concentration of peptide with one metal ion bound, and $[PM_2]$ = concentration of peptide with two metal ions bound.

The observed chemical shift at each point in the titration is given by

$$\delta_{obsd} = f_P\delta_P + f_{PM}\delta_{PM} + f_{PM_2}\delta_{PM_2} \quad (3)$$

where δ_{obsd} represents the chemical shift of a peptide resonance at a particular point of the titration, δ_P represents the resonance position in the absence of metal, δ_{PM} represents the chemical shift of the 1:1 peptide–metal complex, δ_{PM_2} represents the chemical shift of the 1:2 peptide–metal complex, and f_P, f_{PM}, and f_{PM_2} are the fractional amounts of each component.

Substituting for

$$f_P = 1 - f_{PM} - f_{PM_2} \quad (4)$$

we obtain

$$\delta_{obsd} = (1 - f_{PM} - f_{PM_2})\delta_P + f_{PM}\delta_{PM} + f_{PM_2}\delta_{PM_2} \quad (5)$$

and rearranging we obtain

$$\delta_{obsd} - \delta_P = f_{PM}(\delta_P - \delta_{PM}) + f_{PM_2}(\delta_{PM_2} - \delta_P) \quad (6)$$

This equation can be rewritten as

$$\delta_{obsd} - \delta_P = ([PM]\Delta_{PM} + [PM_2]\Delta_{PM_2})/[P_0] \quad (7)$$

where Δ_{PM} is the difference in chemical shifts of a resonance in the 1:1 peptide–metal and metal-free forms and Δ_{PM_2} is the difference in chemical shifts of a resonance in the 1:2 peptide–metal and metal-free forms. This equation contains two unknown concentrations, [PM] and $[PM_2]$; $[PM_2]$ can be described in terms of [PM] by substituting $[M_0] = [M] + [PM] + 2[PM_2]$ into eq 2 to give

$$K_{d2} = ([M_0] - [PM] - 2[PM_2])[PM]/[PM_2] \quad (8)$$

Rearrangement gives

$$[PM_2] = [PM]([M_0] - [PM])/(2[PM] + K_{d2}) \quad (9)$$

Equation 7 can then be written as

$$\delta_{obsd} - \delta_P = \{([PM]\Delta_{PM}) + \{[PM]([M_0] - [PM])/(2[PM] + K_{d2})\}\Delta_{PM_2}\}/[P_0]$$

The value of [PM] is given by the root of a cubic equation (*Handbook of Physics and Chemistry*, 1962–1963; Williams et al., 1985):

$$[PM] = 2(A/3)^{1/2} \cos[(\theta/3) + 240°] - P_0/3$$

where

$$\theta = \arccos[(-B/2)/[(-A^3)^{1/2}/27]]$$

$$A = (1/3)(3Q - P^2)$$

$$B = (1/27)(2P^3 - 9PQ + 27R)$$

$$P = (K_{d2}^2 - 4K_{d1}K_{d2} - 2M_0K_{d2})/(K_{d2} - 4K_{d1})$$

$$Q = (2M_0P_0K_{d2} - P_0K_{d2}^2 - K_{d1}K_{d2}^2 - M_0K_{d2}^2 - M_0^2K_{d2})/(K_{d2} - 4K_{d1})$$

$$R = (P_0M_0K_{d2}^2)/(K_{d2} - 4K_{d1})$$

and P_0 = total concentration of peptide in the complex, M_0 = total concentration of metal in the complex, K_{d1} = first metal dissociation constant, and K_{d2} = second metal dissociation constant.

A least-squares fitting procedure was used to determine the values of the La^{3+} affinity constant (K_{d1}), the chemical shift of the 1:1 peptide–metal complex (Δ_{PM}), and the chemical shift of the 1:2 peptide–metal complex (Δ_{PM_2}). The association constant for the interaction with the second metal ion was set to 10^2 M^{-1} in all cases. This is the value that was determined for the binding of La^{3+} to the acetate ion (Kolat & Powell, 1962). When this constant was well determined it was in this range; but for most plots this affinity was not well determined. Fixing the value for this constant at 10^2 M^{-1} greatly improved the accuracy and reliability of the determination of the other parameters. The interaction of this second La^{3+} ion is most likely to occur at Glu-113, which is not involved in the coordination of the first La^{3+} ion. The experimental data used for this calculation were the chemical shift ratio (CSR), which was determined from as many resonances as possible, and the concentrations of the peptide and La^{3+} ion used in the titration. The CSR is calculated as

$$CSR = (\delta_{obsd} - \delta_F)/(\delta_S - \delta_F)$$

where δ_S represents the chemical shift of a peptide resonance at a 1:1 peptide–metal ratio, δ_{obsd} is the observed chemical shift value for the same resonance at a particular point of the titration, and δ_F represents the resonance position at the start of the titration in the absence of metal.

Calculation of the Free Energy Contributions of Asp Residues to the La^{3+}-Binding Affinity of the Synthetic Analogues. These calculations were performed by assuming that

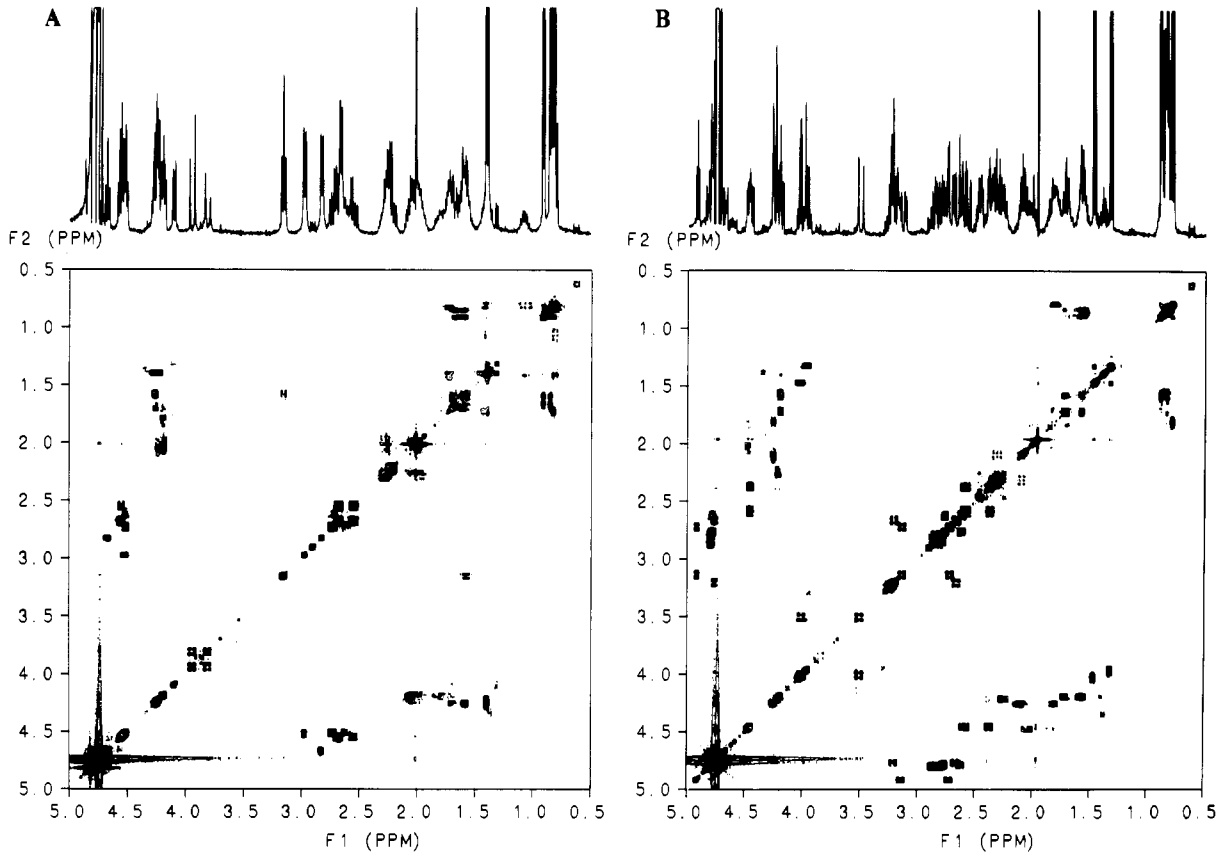

FIGURE 1: Two-dimensional (2D) COSY spectra of the apo (A) and metal-saturated (B) forms of peptide N [AcSTnC(103–115)amide]; above each 2D plot is shown the corresponding 1D plot. The spectra shown are for a different sample than that used for determination of the association constant. [Peptide] = 1.83 mM in 100 mM KCl, [La^{3+}] = 9.14 mM, pH 6.50. COSY (B) of the metal-saturated form clearly shows large shifts induced by La^{3+} binding for the Gly-108 α-CH_2 resonances to 3.5 and 4.0 ppm, also for the Asp-103, -107, and -111 and Asn-105 β-CH_2 resonances (in the region 2.3–3.0 ppm), and the separation of the Ala-106 and -112 β-CH_3 resonances to 1.3 and 1.4 ppm.

the only contributions to the change in La^{3+}-binding affinity resulting from substitution of Asn residues by Asp at the liganding positions were due to contributions to dentate–ligand interactions and to dentate–dentate repulsion between Asp residues at either the +X and +Y, +Y and +Z, or +X and +Y and +Z positions. The equation used for these calculations was

$$\Delta\Delta G = \Delta G_1 - \Delta G_2 = -RT(\ln K_1 - \ln K_2) = -RT \ln (K_1/K_2)$$

where $\Delta\Delta G$ is the difference in Gibbs free energy between ΔG_1, that of the peptide with an Asn at a particular position, and ΔG_2, that produced by substitution of the Asn residue by an Asp residue, R is the gas constant, T is the temperature in Kelvin, and K_1 is the association constant for peptides N and I–VI and K_2 that for peptide VII.

RESULTS

Assignment of the Peptide Resonances. The sequences of the peptides are given in Table I. As can be seen, there are two alanines, two glutamic acids, from one to four aspartic acids, and from zero to three asparagines. This complexity affects the assignment of the residues, as does the overlap of the arginine, leucine, and isoleucine methylene protons, and also the overlap of the tyrosine and aspartic acid/asparagine β-methylene protons.

The initial assignments of the spectra of the apopeptides were made by using the published list of proton NMR resonances recorded for synthetic peptides containing each amino acid (Bundi & Wuthrich, 1979) and from 2D correlated (COSY) spectra [Figure 1 shows two COSY spectra of the apo (A) and La^{3+}-bound (B) forms of the peptide with the native sequence]. Several assignments were made easily, such as the aromatic protons of the tyrosine at 6.8 and 7.0 ppm, the glycine α-CH_2 protons near 3.9 ppm, the *N*-acetyl methyl protons at ~2.0 ppm, and the alanine, leucine, and isoleucine methyl protons. The COSY of the metal-saturated peptide was invaluable in helping to assign many of the resonances,

Table I: Sequences of Synthetic Analogues of Site III of Rabbit Skeletal Troponin C

1[a] 2 3 4 5 6 7 8 9 10 11 12 103[b] 105 107 109 111 114 X[d] Y Z -Y -X -Z	Peptide[c]	Number of Charged Ligands
Ac-**Asp**-Arg-**Asn**-Ala-**Asp**-Gly-**Tyr**-Ile-**Asp**-Ala-Glu-**Glu**-Leu-NH_2	N	4
Ac-**Asp**-Arg-<u>Asp</u>-Ala-**Asp**-Gly-**Tyr**-Ile-**Asp**-Ala-Glu-**Glu**-Leu-NH_2	I[e]	5
Ac-<u>Asn</u>-Arg-<u>Asp</u>-Ala-**Asp**-Gly-**Tyr**-Ile-**Asp**-Ala-Glu-**Glu**-Leu-NH_2	II	4
Ac-**Asp**-Arg-<u>Asp</u>-Ala-<u>Asn</u>-Gly-**Tyr**-Ile-**Asp**-Ala-Glu-**Glu**-Leu-NH_2	III	4
Ac-**Asp**-Arg-**Asn**-Ala-<u>Asn</u>-Gly-**Tyr**-Ile-**Asp**-Ala-Glu-**Glu**-Leu-NH_2	IV	3
Ac-<u>Asn</u>-Arg-**Asn**-Ala-**Asp**-Gly-**Tyr**-Ile-**Asp**-Ala-Glu-**Glu**-Leu-NH_2	V	3
Ac-<u>Asn</u>-Arg-<u>Asp</u>-Ala-<u>Asn</u>-Gly-**Tyr**-Ile-**Asp**-Ala-Glu-**Glu**-Leu-NH_2	VI	3
Ac-<u>Asn</u>-Arg-**Asn**-Ala-<u>Asn</u>-Gly-**Tyr**-Ile-**Asp**-Ala-Glu-**Glu**-Leu-NH_2	VII	2

[a] Position within the calcium-binding loop region. [b] Position in the sequence of rabbit skeletal troponin C. [c] Peptide N is AcSTnC(103–115)amide, peptide I is Ac(Asp-105)STnC(103–115)amide, peptide II is Ac(Asn-103,Asp-105)STnC(103–115)amide, peptide III is Ac(Asp-105,Asn-107)STnC(103–115)amide, peptive IV is Ac(Asn-107)STnC-(103–115)amide, peptide V is Ac(Asn-103)STnC(103–115)amide, Peptide VI is Ac(Asn-103,Asp-105,Asn-107)STnC(103–115)amide, and peptide VII is Ac(Asn-103,Asn-107)STnC(103–115)amide. [d] The letters X, Y, Z, -Y, -X, and -Z represent the calcium-coordinating positions of the peptide. [e] The underlined residues denote changes from the native sequence.

Table II: Assignment of the ^1H NMR Resonances of the Apo-AcSTnC(103–115)amide Analogues

	resonance position (ppm)	resonance pattern obsd	proton assignment
A[a]	0.76–0.87	multiplet (doublet and triplet)	δ-CH_3, Leu-115
			δ-CH_3, Ile-110
	0.87	doublet	γ-CH_3, Ile-110
	0.90	doublet	δ-CH_3, Leu-115
	1.05–1.10	complex multiplet	γ-CH_2, Ile-110
B	1.35–1.40	doublet	β-CH_3, Ala-106, -112
		complex multiplet	γ-CH_2, Ile-110
C	1.65–1.90	complex multiplets	γ-CH_2, Arg-104
			β-CH, Ile-110
			β-CH_2, Leu-115
			β-CH_2, Arg-104
			γ-CH, Leu-115
D	2.00	singlet	*N*-Ac, Asp-103
	1.95–2.05	complex multiplet	β-CH_2, Glu-113, -114
E	2.20–2.30	complex multiplet	γ-CH_2, Glu-113, -114
F	2.50–2.80	complex multiplets	β-CH_2, Asp-111, Asx-103, -105, -107
G	2.95–3.00	"doublet"	β-CH_2, Tyr-109
H	3.10–3.15	triplet	δ-CH_2, Arg-104
I	3.80–4.00	singlet or quartet	α-CH_2, Gly-108
J	4.05–4.10	doublet	α-CH, Ile-110
K	4.20–4.40	complex multiplets	α-CH, Glu-113, -114
			α-CH, Ala-106, -112
			α-CH, Arg-104
			α-CH, Leu-115
L	4.50–4.80	complex multiplets	α-CH, Tyr-109
			α-CH, Asp-111
			α-CH, Asx-103, -105, -107
	6.80–6.90	doublet	ring, aromatic 3,5 Tyr-109
	7.00–7.10	doublet	ring, aromatic, 2,6 Tyr-109

[a] The letters refer to regions of the spectra highlighted in Figure 2a.

as can be seen in Figure 1B for the region 2.0–3.3 ppm, which includes the Asp and Tyr β-methylene protons. Not all of the resonances were assigned because of the severe overlap of some of the resonances and because of broadening that occurred during the early parts of the titration. The assigned resonances are listed in Table II.

A comparison of the spectra of all the apopeptides (Figure 2a) showed that they were all very similar, with most resonances having very similar chemical shifts in each of the peptides. One of the most apparent differences was those of the Gly-108 α-protons (3.7–4.0 ppm), which were magnetically equivalent and yield a singlet in some peptides (peptides I and III, Figure 2a), but in the other peptides they were magnetically inequivalent, giving rise to a characteristic AB quartet (highlighted for the native sequence N, Figure 2a). The superposition of the alanines and the fact that most of the resonances had similar chemical shifts to those reported for the model tetrapeptides would indicate that these peptides possess little secondary structure as reported by Gariépy et al. (1983).

Lanthanide Titrations. The La^{3+} ion used for the titrations is expected to produce no paramagnetic shifting or broadening of the peptide ^1H NMR resonances, as the ion is diamagnetic and has no unpaired electrons. Therefore, the observed perturbations observed in the ^1H NMR spectra are due to changes in conformation resulting from La^{3+} ion binding or small inductive effects on the resonances of the liganding residues. As can be seen from a comparison of the ^1H NMR spectra of the apopeptides (Figure 2a) and those taken at La^{3+}/peptide ratios of 1:1 (Figure 2b), many of the resonances undergo considerable chemical shift changes. The largest chemical shift change observed for each of the analogues was usually that of the glycine α-protons; the chemical shift separation of the resonances for the two protons usually increased upon metal binding (compare highlighted resonances for peptide N in panels a and b of Figure 2). This suggests that the conformation in the vicinity of Gly-108 changes in such a way that the two α-protons are made more nonequivalent relative to the shielding effects of the aromatic ring of Tyr-109 or neighboring carbonyl groups. On the other hand, in peptide V the glycine quartet in the apopeptide (Figure 2a) collapses to a singlet in the La^{3+}-bound peptide (Figure 2b). Another obvious changes occurs for the two alanine methyl resonances, which are superimposed in the apopeptides (doublet at 1.4 ppm) but separate upon the addition of La^{3+}. These spectral changes indicate that structural changes have occurred upon binding of La^{3+}. The largest chemical shift changes are observed for those peptides that have the highest La^{3+} affinities, indicating that these peptides undergo the largest conformational changes.

Table III: La^{3+} Association Constants for Synthetic Analogues of Rabbit Skeletal Troponin C

analogue[a]	coordinating positions X	Y	Z	no. of charged ligands	association const (M^{-1})
I	Asp	Asp	Asp	−5	1.4×10^5
N	Asp	Asn	Asp	−4	2.5×10^5
II	Asn	Asp	Asp	−4	5.3×10^4
III	Asp	Asp	Asn	−4	1.8×10^4
IV	Asp	Asn	Asn	−3	2.4×10^3
V	Asn	Asn	Asp	−3	1.6×10^4
VI	Asn	Asp	Asn	−3	1.5×10^4
VII	Asn	Asn	Asn	−2	9.1×10^2

[a] Primary sequences of the analogues are given in Table I.

^1H NMR spectra were recorded at many points during the course of the lanthanum titration; Figure 3 shows a portion of the α-CH region of the spectra recorded for the La^{3+} titration of peptide II. The changes in chemical shift were recorded for as many resonances as possible; however, this was complicated due to the severe overlap that occurred, particularly in the β- and γ-methylene proton region (1.5–3.0 ppm) and also due to exchange broadening that occurred between the La^{3+} to peptide ratios of 0–1:1. At the completion of the La^{3+} titration another COSY spectrum was recorded to further aid in the assignment of resonances (see Figure 1).

Lanthanum Binding Constants. The chemical shift ratio was determined for as many resonances of each analogue as possible; this value was then plotted against the La^{3+}/peptide ratio. Figure 4 shows the plots obtained for some of the α-CH protons of peptide II that are indicated in Figure 3; these are typical of the curves obtained from other resonances of this and the other analogues. The curves of the higher affinity analogues show that a maximal chemical shift is reached at a La^{3+}/peptide ratio of 1:1, indicating a stoichiometry of 1:1. The titration plots of some of the resonances provided evidence for the interaction of a second La^{3+} ion as these plots showed that further changes in chemical shift occurred as excess La^{3+} was added. The interaction of a second La^{3+} ion was included in the equation for calculating the La^{3+} binding constants as described under Experimental Procedures; the association constant ascribed for this interaction was 10^2 M^{-1}. This is the value that was determined for the binding of La^{3+} to the acetate ion (Kolat & Powell, 1962). Figure 5 depicts the plots obtained for the same α-proton of Gly-108 of peptides N, III, IV, and VII. These curves indicate the wide range of affinities observed for the eight analogues; the affinities were calculated as described under Experimental Procedures and are given in Table III.

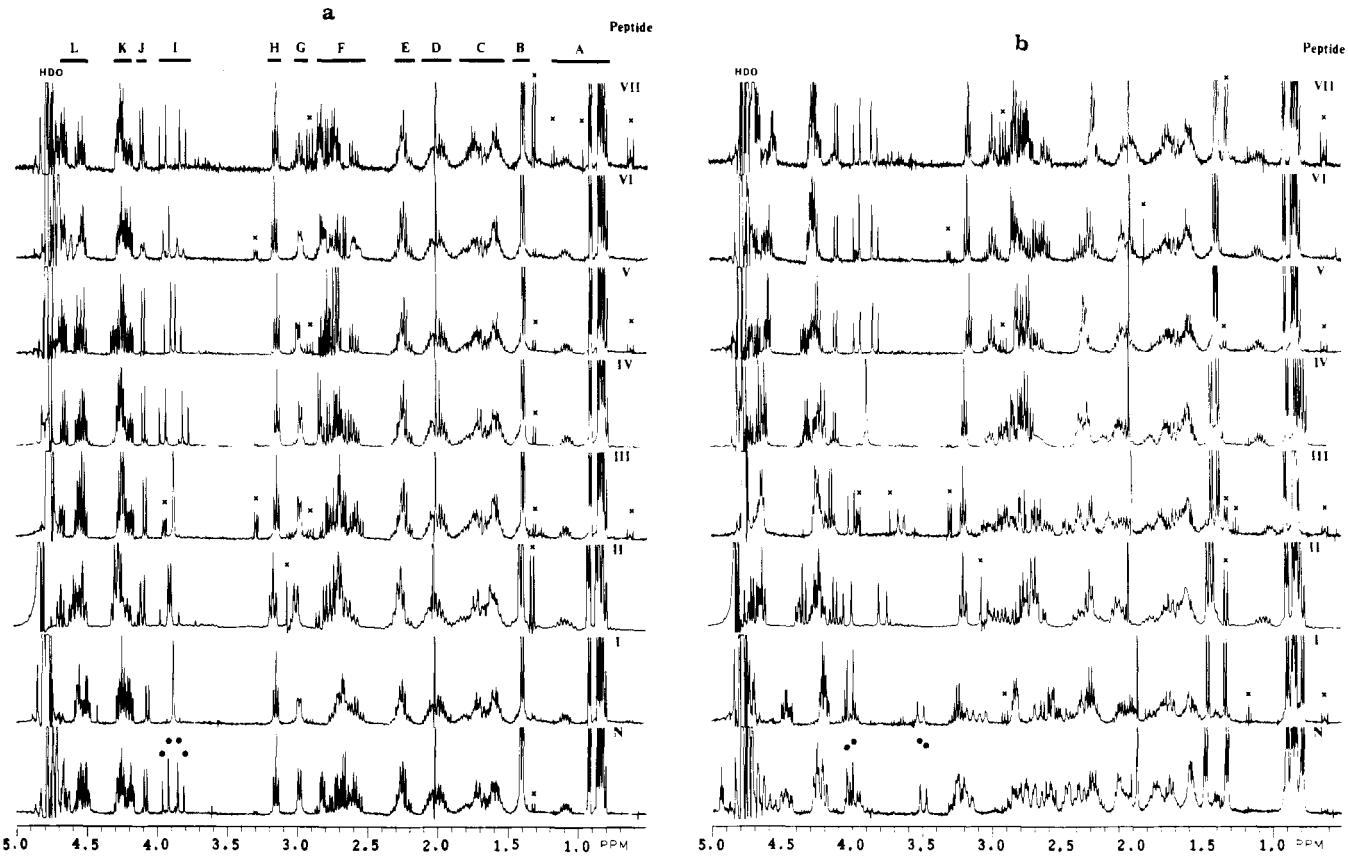

FIGURE 2: (a) ^1H NMR spectra of the apopeptides (the aliphatic region is shown). Peptide concentrations and conditions are given under Experimental Procedures. The assignment of the resonances in regions of the spectra A–L are given in Table II. The resonances highlighted with the symbol × denote impurities or peaks due to DSS, and those highlighted with the symbol • are the Gly-108 α-CH_2 protons described under Results. (b) ^1H NMR spectra of the peptides at a La^{3+}/peptide ratio of approximately 1:1. All titrations were performed beyond a La^{3+}/peptide ratio of 4:1. The resonances highlighted with the symbol × denote impurities or peaks due to DSS, and those highlighted with the symbol • are the Gly-108 α-CH_2 protons described under Results.

DISCUSSION

Synthetic peptides were first used by Hodges and co-workers to probe the local molecular events that occur within a Ca^{2+}-binding site upon binding metal ions (Reid et al., 1980, 1981; Gariépy et al., 1983). By use of a series of synthetic peptides, up to 34 residues in length, it was shown that the C-terminal and N-terminal helices stabilize the Ca^{2+}-binding unit and that the Ca^{2+}-induced helix was in the N-terminal region of the helix–loop–helix structure. In addition, these researchers showed that the Ca^{2+}-binding loop region itself could bind metal ions and that the amino acid sequence within the loop controlled metal ion selectivity (Reid et al., 1980; Gariépy et al., 1983). Although many workers have since used synthetic peptides to study metal ion binding (Kanellis et al., 1983; Marchiori et al., 1983; Pavone et al., 1984; Borin et al., 1985; Buchta et al., 1986; Malik et al., 1987), this is the first study using synthetic peptides to systematically examine the effect of the number and position of charged ligands in the coordinating positions of Ca^{2+}-binding sites.

We have synthesized eight analogues which represent all the permutations having Asp and Asn residues at the +X, +Y, and +Z metal-coordinating positions. The La^{3+} affinity constants for these peptides (Table III) show a general increase as the number of Asp residues at the +X, +Y, and +Z positions is increased from 0 to 3. The exception to this trend is peptide I, which was five acidic ligands (Asp residues at each of the +X, +Y, and +Z positions). This analogue has a La^{3+} affinity slightly lower than that of peptide N (1.4×10^5 M^{-1} and 2.5×10^5 M^{-1}, respectively), which only has four acidic ligands (Asp residues at the +X and +Z positions). This observation provides experimental evidence to support a postulate made by Reid and Hodges: that calcium-binding loops which have Asp residues at either the +X and +Y or the +Y and +Z positions would result in dentate–dentate repulsion, thereby lowering the metal ion affinity as compared to loops in which this dentate–dentate repulsion does not occur. Peptide I has Asp residues at each of the +X, +Y, and +Z positions, thus giving rise to both of these unfavorable dentate–dentate interactions. The absence of these dentate–dentate repulsions also helps to explain why peptide N has a higher La^{3+} affinity than do peptides II and III, which also have four acidic ligands, but one of the unfavorable dentate–dentate interactions, the +X and +Y interaction for peptide III and the +Y and +Z interaction for peptide II.

For the purpose of quantitative comparison peptide VII, the analogue with three Asn residues at the positions of study, can be considered as the basis from which all the others are derived by substitution of Asp residues for Asn. Peptide VII has only three Asn residues and the two conserved acidic ligands at the −X and −Z positions to coordinate the La^{3+} ion and, as would be expected, has the lowest La^{3+} affinity of the analogues studied, 9.1×10^2 M^{-1}. Substitution of any one of the Asn residues of peptide VII by an Asp yields analogues with three acidic ligands; peptide IV has that Asp at the +X position, peptide V at the +Z position, and peptide VI at the +Y position. Analysis of the La^{3+} affinity of these analogues can be used to determine the contribution of an Asp residue at each of these positions. The La^{3+} affinity of these analogues are 2.4×10^3 M^{-1} for peptide IV, 1.6×10^4 M^{-1} for peptide V, and 1.5×10^4 M^{-1} for peptide VI. These results indicate that introduction of an Asp residue at either the +Y or +Z position increases the La^{3+} affinity of the respective peptides by a factor of ~17, whereas introduction of an Asp residue at the +X position increases the La^{3+} affinity by a factor of only ~2.

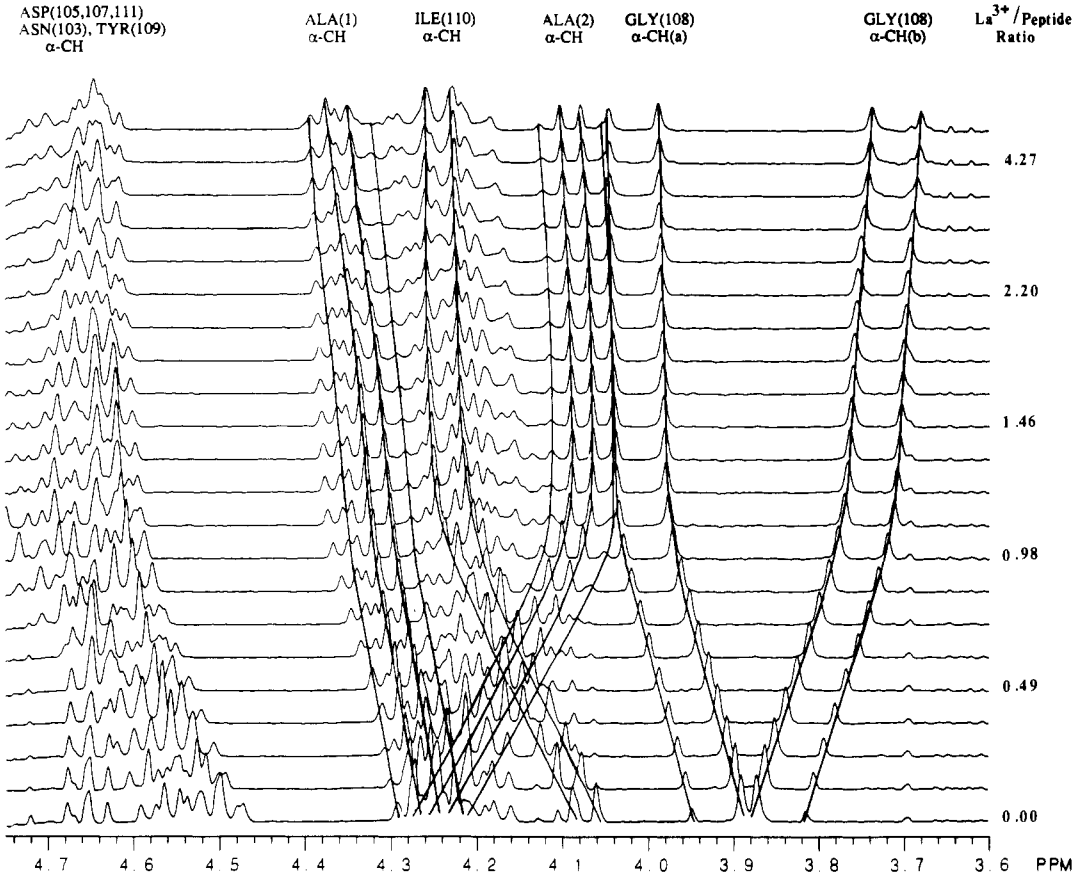

FIGURE 3: Lanthanum titration of peptide II [Ac(Asn-103,Asp-105)STnC(103–115)amide]. [Peptide] = 1.88 mM, [La^{3+}] = 0.00, 0.12, 0.24, 0.37, 0.49, 0.61, 0.73, 0.85, 0.98, 1.10, 1.22, 1.34, 1.46, 1.59, 1.71, 1.95, 2.20, 2.44, 3.05, 3.66, 4.27, and 4.88 mM in 100 mM KCl, pH 6.50. The spectra show the α-CH region. The resonances highlighted by continuous lines are some of those used to determine the La^{3+} affinity of this peptide.

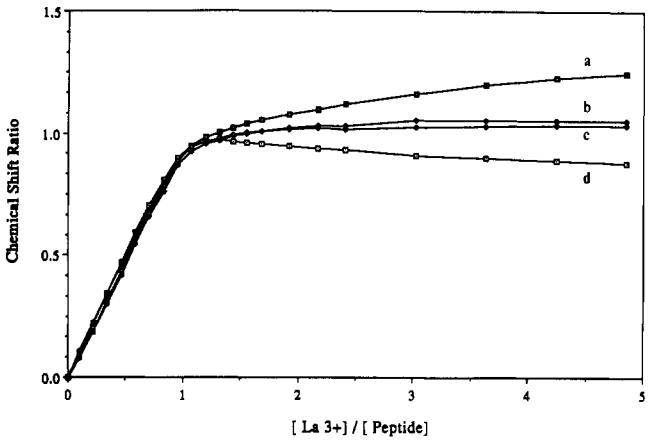

FIGURE 4: Lanthanum titration plots of peptide II [Ac(Asp-103,Asp-105)STnC(103–115)amide]. The plots shown are for some of the resonances highlighted in Figure 3: (a) Ala-1, (b) Gly (a), (c) Gly (b), and (d) Ile. The observed chemical shift ratio (CSR) has been normalized for a La^{3+}/peptide ratio of 1:1.

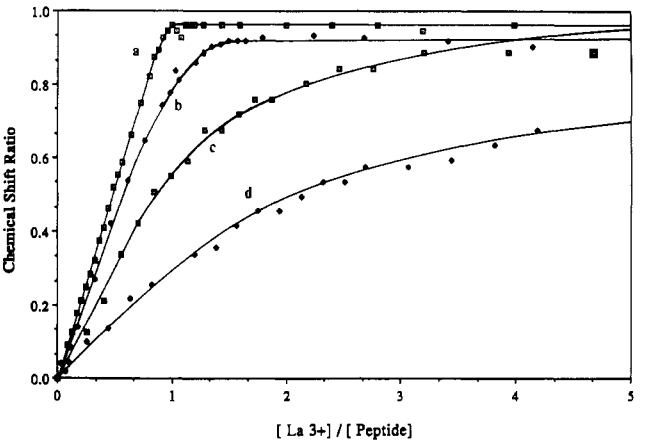

FIGURE 5: Lanthanum titration plots of peptides N, III, IV, and VII. The plots shown are for the downfield shifting Gly-108 α-CH resonance: (a) peptide N, (b) peptide III, (c) peptide IV, and (d) peptide VII. Experimental conditions are given under Experimental Procedures. The observed chemical shift ratio (CSR) has been normalized for a La^{3+}/peptide ratio of 1.

The reduced contribution of the Asp residue at the +X position is possibly due to the magnitude of the peptide–La^{3+} interaction at the +Y and +Z positions (both dentates at the +Y and +Z positions are the neutral carbonyl oxygen atoms of the Asn side chains) not being large enough to hold the peptide in a conformation that would allow a strong interaction between the oxygen atoms of the negatively charged Asp residue at the +X position and the La^{3+} ion.

There are also three analogues with four acidic ligands: peptide N has Asp residues at the +X and +Z, peptide II at the +Y and +Z, and peptide III at the +X and +Y positions. The La^{3+} affinity of these peptides are $\sim 2.5 \times 10^5$ M^{-1}, 5.3×10^4 M^{-1}, and 1.8×10^4 M^{-1}, respectively. The La^{3+} affinity of the native sequence is larger than that determined by Gariépy et al. (1983), who reported a value of 1.1×10^5 M^{-1}; this difference between the two results can be ascribed to the different pH values used for the two studies. This study was performed at a pH of 6.50 whereas that of Gariépy et al. was performed at a pH of 6.00. The La^{3+} affinity of these analogues is higher than those observed for the analogues with three acidic ligands. These analogues also allow the contribution of substituting a further Asp for Asn residue into the sequence of peptides IV–VI (which have three acidic ligands)

Table IV: Free Energy Contributions to the La^{3+} Association Constants for Substitution of Asn by Asp

peptide[a]	position of Asp residue			model A[b]						model B[c]						
				$\Delta\Delta G$			$\Delta\Delta G_r$[e]			$\Delta\Delta G$			$\Delta\Delta G_r$			
	+X	+Y	+Z	X	Y	Z	XY	YZ	calcd $\Delta\Delta G$	X	Y	Z	XY	YZ	calcd $\Delta\Delta G$	obsd[d] $\Delta\Delta G$
VII	–	–	–	0	0	0	0	0	0	0	0	0	0	0	0	0
IV	+	–	–	−2.5	0	0	0	0	−2.5	−7.1	0	0	0	0	−7.1	−2.5
VI	–	+	–	0	−7.1	0	0	0	−7.1	0	−7.1	0	0	0	−7.1	−7.1
V	–	–	+	0	0	−7.1	0	0	−7.1	0	0	−7.1	0	0	−7.1	−7.1
III	+	+	–	−2.5	−7.1	0	+4.1	0	−5.5	−7.1	−7.1	0	+4.1	0	−10.1	−7.4
II	–	+	+	0	−7.1	−7.1	0	+4.1	−10.1	0	−7.1	−7.1	0	+4.1	−10.1	−10.1
N	+	–	+	−2.5	0	−7.1	0	0	−7.6	−7.1	0	−7.1	0	0	−14.2	−13.9
I	+	+	+	−2.5	−7.1	−7.1	+4.1	+4.1	−8.5	−7.1	−7.1	−7.1	+4.1	+4.1	−13.1	−12.5

[a] The primary sequence of the peptides is given in Table I. [b] In this model the free energy contribution of an Asp residue at the +X position is set to -2.5×10^3 J mol^{-1}, as determined from peptide IV. [c] In this model the free energy contribution of an Asp residue at the +X position is set to -7.1×10^3 J mol^{-1}, as is used for an Asp residue at the +Y and +Z positions. [d] The observed free energies are calculated from the measured affinities as described under Experimental Procedures. [e] The free energy contribution of the dentate–dentate repulsive term ($+4.1 \times 10^3$ J mol^{-1}) is determined as the difference between the calculated contribution from two Asp residues [$2(-7.1 \times 10^3$ J $mol^{-1})$] and that observed for peptide II (-10.1×10^3 J mol^{-1}).

to be determined. Each of the peptides with four acidic ligands may be derived from the peptides with three acidic ligands (peptides IV–VI) in two ways. Peptide N can be obtained by a substitution of the Asn residue for an Asp at the +X position of peptide V or at the +Z position of peptide IV, peptide II by similar substitutions at the +Y position of peptide V or at the +Z position of peptide VI, and peptide III by substitutions at the +Y position of peptide IV or at the +X position of peptide VI. Substitution of the Asn residue at the +X position of peptide VI by an Asp residue to produce peptide III increases the La^{3+} affinity only slightly from 1.5×10^4 M^{-1} to 1.8×10^4 M^{-1}. The explanation for this smaller than expected increase in affinity may be due to dentate–dentate repulsion between the Asp residues at the +X and +Y positions and may also be due in part to the observation made for the analogues with three acidic ligands: that the Asp residue at the +X position does not coordinate with the La^{3+} efficiently (as was found for peptide IV, which has the lowest La^{3+} affinity of the analogues with three acidic ligands). Comparing peptide III to peptide IV shows an increase in La^{3+} affinity to 1.8×10^4 M^{-1} from 2.4×10^3 M^{-1}. This 9-fold increase in affinity is less than that expected for the introduction of an Asp residue at a liganding position and may be ascribed to dentate–dentate repulsion between the Asp residues as described earlier. The La^{3+} affinity of peptide II is 5.3×10^4 M^{-1}, which is approximately 3 times greater than those of peptides V and VI, 1.6×10^4 M^{-1} and 1.5×10^4 M^{-1}, respectively. This increase in affinity is lower than that expected for the introduction of a liganding Asp residue and is also ascribed to dentate–dentate repulsion between the Asp residues at the +Y and +Z positions.

Peptide N can be derived from peptides IV and V by substitution at the +Z position of peptide IV or at the +X position of peptide V. The La^{3+} affinity of peptide N is 2.5×10^5 M^{-1}, which is a 125-fold increase in affinity over that of peptide IV; this increase is much larger than the 17-fold increase expected and can be explained in terms of increased efficiency in liganding by the Asp residue at the +X position brought about by the substitution of the Asn residue by Asp at the +Z position. The increase in La^{3+} affinity of peptide N, 2.5×10^5 M^{-1}, above that of peptide V, 1.6×10^4 M^{-1}, is 16-fold; this is almost the same as the 17-fold increase in affinity observed for the introduction of Asp residues at either the +Y or +Z positions (peptide VII to peptide VI and peptide VII to peptide V, respectively) but is much larger than observed for the introduction of an Asp residue at the +X position compared to the cases discussed earlier, i.e., peptides IV and III.

The data obtained for the analogues with four acidic ligands show that not only is the number of acidic ligands an important factor in determining the affinity but it is also important whether there are dentate–dentate repulsive interactions between Asp residues. These experimental data support another postulate made by Reid and Hodges (1980) that "the calcium-binding loop having the highest metal-binding affinity would have four acidic ligands situated on the ±X and ±Z axes". This proposal was based on the fact that in this arrangement the ligands are at their maximal separation and no dentate–dentate repulsion is expected. In any other arrangement of four acidic ligands there will always be two ligands on neighboring axes in an unpaired fashion, and dentate–dentate repulsion would occur.

The comparisons discussed above can be restated in thermodynamic terms to assess the contributions to the free energy from substitution of Asn residues by Asp at each of the +X, +Y, and +Z positions. The following assumptions were made to allow a comparison of the results: (1) that the conformation of the 1:1 peptide/La^{3+} complex was the same for all the analogues, (2) that the free energy contributions to the La^{3+} affinity of the Asp residues can be combined in a linear fashion, and (3) that dentate–dentate repulsion occurs only between the Asp residues at the +X and +Y and the +Y and +Z positions.

The calculated free energies of the analogues are given in Table IV, in which two models are shown; in model A the contribution of the Asp residue at the +X position is set to -2.5×10^3 J mol^{-1}, the value calculated from the Asn to Asp substitution in peptide VII to peptide IV, whereas in model B this contribution is set to -7.1×10^3 J mol^{-1}, the value calculated for the contribution of the Asp residues at each of the +X, +Y, and +Z positions as determined from the Asn to Asp substitutions in peptides V to N, VII to VI, and VII to V, respectively. The value used for contribution of the dentate–dentate repulsion, $+4.1 \times 10^3$ J mol^{-1}, was determined as the difference between the calculated contribution from two Asp residues and that observed for peptide II. A comparison of the values calculated by using model A and the observed values shows that there are large discrepancies for peptides I and N with a smaller discrepancy for peptide III, whereas a similar comparison using the values calculated with model B reveals a large discrepancy only for peptide IV with a smaller discrepancy, similar to that observed with model A, for peptide III. The results of these comparisons show that better predictions are obtained when the contribution of the Asp residue at the +X position is -7.1×10^3 J mol^{-1} and not the observed value of -2.5×10^3 J mol^{-1}. This indicates that the Asp at the +X position does not ligand the La^{3+} ion efficiently in peptides IV and III, as was discussed previously. The con-

clusions from this analysis are that the contribution of a liganding Asp residue to the La^{3+} affinity is roughly the same when it is at either the +X, +Y, or +Z position.

In this study we have been able to show that the liganding Asp residues at the +X, +Y, and +Z positions within a calcium-binding site contribute equally to the Ca^{2+} affinity of that site. Also, the presence of Asp residues at the +X and +Y, the +Y and +Z, or the +X and +Y and +Z positions introduces dentate–dentate repulsive interactions that act to reduce the metal ion affinity of the site. These conclusions imply that the affinity of a calcium-binding site can be controlled by the ligand sequence within the loop. The composition of 201 naturally occurring loops support this inference. An analysis of the sequence of these calcium-binding loops reveals that there are 14 loops with five acidic ligands,[2] 143 with four acidic ligands, 41 with three acidic ligands, and 3 with two acidic ligands. These data could suggest that loops with five acidic ligands are not favored either because of dentate–dentate repulsion reducing the efficiency of coordination of the Ca^{2+} ion or because of possible unfavorable conformations that dentate–dentate repulsion inflicts upon the loop. There are only 7 of a possible 16 permutations found for loops having either three (3 of 10), four (3 of 5), or five (1) acidic ligands. The ligand sequences for the 41 loops with three acidic ligands are 110001 (21), 101001 (17), and 011001 (3); those for the 143 loops with four acidic ligands are 111001 (61), 110011 (54), and 101011 (28); and that for the 14 loops with five acidic ligands is 111011 (where 1 indicates an acidic ligand and 0 a neutral one). By use of the results of this study the predicted order of affinities of these ligand sequences would be 101001 > 111011 > 110011 > 111001 > 101001 > 110001 = 011001. For this prediction to be tested a similar study to the one described is required for those analogues having the ligand sequences 111001, 101001, 110001, and 011001. For extension of this prediction to the affinities of ligand sequences found in the calcium-binding proteins, and for comparisons between the affinities of the various calcium-binding proteins, more information is required as to how other structural elements of these proteins contribute to the affinity of metal ion binding loops.

ACKNOWLEDGMENTS

We thank Dr. J. M. R. Parker for providing invaluable assistance with the peptide synthesis and purification, M. Nattriss for performing the amino acid analyses of the samples in this study, and Dr. W. Paranchych for use of the HPLC equipment.

Registry No. I, 103974-68-1; II, 103974-67-0; III, 114185-57-8; IV, 114185-58-9; V, 114185-59-0; VI, 114185-60-3; VII, 103974-66-9; N, 84648-71-5; L-Asp, 56-84-8; L-Asn, 70-47-3; La, 7439-91-0.

REFERENCES

Barany, G., & Merrifield, R. B. (1980) in *The Peptides* (Gross, E., & Meienhoffer, J., Eds.) Vol. 2, p 1, Academic, New York.

Barker, W. C., Ketcham, L. K., & Dayhoff, M. O. (1978) in *Atlas of Protein Sequence and Structure* (Dayhoff, M. O., Ed.) Vol. 5, Suppl. 3, p 273, The National Biomedical Research Foundation, Silver Spring, MD.

Borin, G., Pezzoli, A., Marchiori, F., & Peggion, E. (1985) *Int. J. Pept. Protein Res. 26*, 528–538.

Brodin, P., Grundström, T., Hoffman, T., Drakenberg, T., Thulin, E., & Forsén, S. (1986) *Biochemistry 25*, 5371–5377.

Buchta, R., Bondi, E., & Fridkin, M. (1986) *Int. J. Pept. Protein Res. 28*, 289–297.

Bundi, A., & Wuthrich, K. (1979) *Biopolymers 18*, 285–297.

Cheung, W. Y. (1970) *Biochim. Biophys. Acta 38*, 533–538.

Derancourt, J., Haiech, J., & Pechère, J.-F. (1978) *Biochim. Biophys. Acta 532*, 373–375.

Ebashi, S., Kodama, A., & Ebashi, F. (1968) *J. Biochem. (Tokyo) 64*, 465–477.

Gariépy, J., & Hodges, R. S. (1983) *FEBS Lett. 160*, 1–6.

Gariépy, J., Sykes, B. D., Reid, R. E., & Hodges, R. S. (1982) *Biochemistry 21*, 1506–1512.

Gariépy, J., Sykes, B. D., & Hodges, R. S. (1983) *Biochemistry 22*, 1765–1772.

Gariépy, J., Kay, L. E., Kuntz, I. D., Sykes, B. D., & Hodges, R. S. (1985) *Biochemistry 24*, 544–550.

Handbook of Physics and Chemistry (1962–1963) 44th ed., p 320, The Chemical Rubber Publishing Co., Cleveland, OH.

Herzberg, O., Moult, J., & James, M. N. G. (1987) *Methods Enzymol. 139*, 610–632.

Kakiuchi, S., & Yamazaki, R. (1970) *Biochim. Biophys. Acta 41*, 1104–1110.

Kanellis, P., Yang, J., Cheung, H. C., & Lenkinski, R. E. (1983) *Arch. Biochem. Biophys. 220*, 530–540.

Kolat, R. S., & Powell, J. E. (1962) *Inorg. Chem. 1*, 293–296.

Kretsinger, R. H. (1980) *CRC Crit. Rev. Biochem. 8*, 119–174.

Kretsinger, R. H., & Nockolds, C. E. (1973) *J. Biol. Chem. 248*, 3313–3326.

Leavis, P. C., Rosenfeld, S. S., Gergely, J., Grabarek, Z., & Drabikowski, W. (1978) *J. Biol. Chem. 253*, 5452–5459.

Lee, L., & Sykes, B. D. (1980) *Biochemistry 19*, 3208–3214.

Malik, N. A., Anantharamaiah, G. M., Gawish, A., & Cheung, H. C. (1987) *Biochim. Biophys. Acta 911*, 221–230.

Marchiori, F., Borin, G., Chessa, G., Cavaggion, G., Michelin, L., & Peggion, E. (1983) *Hoppe Seyler's Z. Physiol. Chem. 364*, 1019–1028.

Marsden, B. J., Hodges, R. S., & Sykes, B. D. (1987) in *Calcium-Binding Proteins in Health and Disease*, pp 412–414, Elsevier/North-Holland, New York.

McFadden, P. N., & Clark, S. (1986) *J. Biol. Chem. 261*, 11503–11511.

Pavone, P. V., Di Nola, A., Andini, S., Ferrara, L., Di Blasio, B., Benedetti, E., & Pucci, P. (1984) *Int. J. Pept. Protein Res. 23*, 454–461.

Potter, J. D., & Gergely, J. (1975) *J. Biol. Chem. 250*, 4628–4633.

Reid, R. E., & Hodges, R. S. (1980) *J. Theor. Biol. 84*, 401–444.

Reid, R. E., Clare, D. M., & Hodges, R. S. (1980) *J. Biol. Chem. 255*, 3642–3646.

Reid, R. E., Gariépy, J., Saund, A. K., & Hodges, R. S. (1981) *J. Biol. Chem. 256*, 2742–2751.

Satyshur, K. A., Rao, S. T., Pyzalska, D., Drendel, W., Greaser, M., & Sundaralingam, M. (1988) *J. Biol. Chem. 263*, 1628–1647.

Seamon, K. B., & Kretsinger, R. H. (1983) in *Calcium in Biology* (Spiro, T. G., Ed.) p 1, Wiley-Interscience, New York.

Vogt, H.-P., Strassburger, W., Wollmer, A., Fleischhauer, J., Bullard, B., & Mercola, D. (1979) *J. Theor. Biol. 76*, 297–310.

Williams, T. C., Shelling, J. G., & Sykes, B. D. (1985) in *Nato Advanced Study Institute on NMR in the Life Sciences* (Bradbury, E. M., & Nicolini, C., Eds.) p 93, Plenum Press, New York.

[2] B. J. Marsden, R. S. Hodges, and B. D. Sykes, unpublished experiments.